The Influence of Permanganate Enhancement to Graphite on Chemical Structure and Properties of Graphene Oxide Material Generated by Improved Tour Method

Dyah Ayu Fatmawati[1*], Triyono Triyono[1], Wega Trisunaryanti[1***], Haryo Satriya Oktaviano[2,3], and Uswatul Chasanah[1]**

[1]*Department of Chemistry, Faculty of Mathematics and Natural Sciences, Universitas Gadjah Mada, Sekip Utara, 55281 Yogyakarta, Indonesia*

[2]*Department of Chemistry, Faculty of Science and Computer, Universitas Pertamina, Simprug, Kebayoran Lama, Jakarta Selatan, DKI Jakarta, 12220, Indonesia*

[3]*Research & Technology Center, PT. Pertamina (Persero), Sopo Del Tower A, Floor 51, Jl. Mega Kuningan Barat III, Kawasan Mega Kuningan, Jakarta Selatan, DKI Jakarta, 12950, Indonesia*

** **Corresponding author:***

email: dyah.ayu.fatmawati@mail.ugm.ac.id; triyn102@ugm.ac.id**; wegats@ugm.ac.id****

Received: June 30, 2020
Accepted: November 15, 2020

DOI: 10.22146/ijc.57423

Abstract: *Synthesis of graphene oxide (GO) material with variations in permanganate/graphite ratio has been carried out. This research purposes to study the impact of increasing oxidizing agents to graphite on the chemical structure and properties of the GO material produced. All GOs were synthesized using the improved Tour method with three variations of permanganate/graphite ratios of 5, 6, and 7. The results obtained include GO-5, GO-6, and GO-7, respectively, having a d spacing value of 0.843; 0.891; 0.894 nm by XRD analysis and 0.768; 0.756; 0.772 nm by SAED analysis. Based on the FTIR data, all GO materials bring up the peaks of oxygen-functionalized carbon absorption such as O–H, C–H sp^3, C=O, C–O–C of ether and ester, and C-OH for carboxylic acids and alcohols. The oxidation levels (O/C ratio taken from EDX data) of GO-5, GO-6, and GO-7 are 0.67, 0.88, and 1.50, respectively. SEM images display the appearance of an exfoliated layer with a wrinkled and irregular surface. TEM images show thin and transparent layers. The main peaks with the highest absorbance at the wavelength around 230-240 nm, meanwhile the band gap energy produced was 3.53; 3.71; 3.55 eV for GO-5, GO-6, and GO-7, respectively.*

Keywords: *chemical properties; chemical structure; graphene oxide; improved tour method; permanganate/graphite ratio*

■ INTRODUCTION

Graphene is a carbon derivative containing a thin layer of sp^2 hybridized carbon atoms in a honeycomb crystal grid [1]. Graphene displays superior electronic and mechanical characters as well as the electrical conductivity of up to 6000 S cm^{-1}, the thermal conductivity of 5000 W m^{-1} K^{-1}, charge-carrier mobility of 250000 cm^2 V^{-1} s^{-1} at ambient temperature, and a broad theoretical specific surface area of 2630 m^2 g^{-1}. Moreover, graphene is exceptionally translucent, with the absorption of < 2.3% against visible light and even, with Young's modulus of 1 TPa and ultimate strength of 130 GPa, single-layer graphene is the most robust material ever investigated [2]. These distinctive qualities of graphene could bring out great implementations as batteries [3], sensors [4], electrochemical supercapacitors [5], electrocatalysis [6], polymer solar cells [7], etc.

Some methods have been declared for the synthesis of graphene that can be principally divided into two diverse ways: the bottom-up [8] and top-down [9] ways. The bottom-up growth of graphene layers is an option for the mechanical exfoliation of bulk graphite. In bottom-up processes, graphene is prepared by a type of

methods like chemical vapor deposition (CVD) and epitaxial growth on SiC. Both of them regularly generate big-sized, lack free graphene in a small amount appropriate for basic research and electronic performances. They are over interesting than the mechanical cleavage method [10]. Nevertheless, these and other methods called before are not compatible with the synthesis of graphene required to prepare graphene-based nanocomposites that generally need significant quantities of graphene layers worthy of a functionalized surface formation. Accordingly, for the fabricating of graphene-based nanocomposites, which mostly involves bulk amounts of homogeneously disparted graphene layers, the top-down way (i.e.) chemical and, or thermal reduction of graphite derivatives such as graphite oxide (GO) emerges to be the supremely convenient and expeditious device [2].

GO is a precursor for graphene synthesis, which is oxygen loaded carbonaceous layered material highly identical to graphite [11]. However, graphite composes simply sp^2 hybridized carbon atoms, while GO includes both sp^3 and sp^2 hybridized carbon atoms. The sp^3 hybridized carbon atoms in GO are covalently bonded with oxygen functional groups as well as carboxyl, epoxy, hydroxyl, etc. [12]. In graphite, two-dimensional layers are organized with each other under weak van der Waals interactions [13]. Nevertheless, whether of GO, the layers are detached by epoxy and water molecules amongst the layers. Consequently, the interlayer spacing of GO is much wider contrasted to graphite [14].

GO has been notably resulted by several differences of Brodie, Staudenmaier, and Hummers methods that implicate the oxidation of graphite in the attendance of strong acids (nitric acid or sulfuric acid) and an oxidizing agent ($KMnO_4$, $KClO_3$, $NaNO_3$). Many different slightly modified and improved versions have also been expanded, including the Tour method [15]. Notably, it has been established that the structure and properties of GO, especially turn on three parameters: the typical synthesis methods, the level of oxidation, and the raw material of graphite utilized.

In this section, throughout their work on the influence of oxidation on the morphology of GO, Lojka and co-workers have noticed cracks in GO that were immediately concerned with the oxidation process. In particular, a few variations in the level of oxidation can lead to significant modifications in the structure and nature of the materials [16]. Hence, in the current work, we will investigate the influence of adding permanganates as oxidants on the structure and properties of GO produced by the improved Tour method.

■ EXPERIMENTAL SECTION

Materials

All materials utilized in this experiment were from commercial sources (E-Merck Germany) and were implemented without the subsequent purification. Materials used involved graphite powder, potassium permanganate ($KMnO_4$, p.a.), sulfuric acid (H_2SO_4 98%, p.a.), ortho-phosphoric acid (H_3PO_4 85%, p.a.), hydrogen peroxide (H_2O_2 30%, p.a.), hydrochloric acid (HCl 37%, p.a.), absolute ethanol (p.a.), silver nitrate (p.a.), and barium chloride (p.a.). For washing the GO solution, deionized (DI) water, phosphate-buffered saline (PBS), and bi-distilled water were utilized.

Instrumentation

X-Ray Diffraction (XRD, Bruker D2 Phaser) at a wide angle of 5–90° was used to determine the crystallinity of the materials. The functional groups of the materials were characterized by Fourier Transform Infra-Red Spectrometer (FTIR, Shimadzu Prestige 21) at 4000–400 cm^{-1}. The structure and polycrystalline ring images of the materials were taken using a Transmission Electron Microscope-Selected Area Electron Diffraction (TEM-SAED, JEOL JEM-1400). The surface morphology and metal content of the materials were evaluated by Scanning Electron Microscope-Energy Dispersive X-ray (SEM-EDX, JSM-6510LA). The wavelength absorption of the materials was observed using UV-Visible Spectrophotometer (UV-Vis, UV-1800 Shimadzu) at a wavelength of 200–800 nm.

Procedure

Our method was taken from Ranjan and co-workers [17] with a few modifications. In the beginning,

potassium permanganate to graphite powder in various ratios of 5, 6, 7 were combined and mashed up homogeneously. The mixture was placed into Beaker A, and the mixture of sulfuric acid and ortho-phosphoric acid in a ratio of 9 was put into Beaker B. The two beakers were kept at a temperature below 5 °C for 6 h. The solution in beaker B was then poured into beaker A and stirred until the solution was greenish-black, later heated at 65 °C for 24 h. After the heating time was finished, the color of the solution became brownish, the beaker left until it reached room temperature. The solution was poured into another beaker containing 500 g of deionized water ice, added with 7 mL of hydrogen peroxide, and stirred using a stirring rod. Instantly, the color of the solution became golden yellow, marking the formation of GO. The solution was left to precipitate the solids GO. GO was washed by centrifugation at 5000 rpm for 5 min using a solution of hydrochloric acid (2 times), ethanol absolute (3 times), and phosphate-buffered saline (PBS) until the pH of the solution became 7. PBS was used to make the washing process more efficient, so it did not need a lot of bi-distilled water. The solution was then checked for chloride ions content using silver nitrate and barium chloride for sulfate ions content. The washing process using bi-distilled water was repeated several times until the solution was free from both of them. The GO solids obtained were dried in an oven, then characterized using XRD, FTIR, SEM-EDX, TEM-SAED, and UV-Visible Spectrophotometer.

■ RESULTS AND DISCUSSION

X-ray Diffraction Analysis

The diffractogram of each GO material is shown in Fig. 1. The graphite shows a sharp and narrow central peak at 2θ = 26.213° originated from the hkl plane of 002 and a very weak peak at 2θ = 42.327° originated from the hkl plane of 100. This corresponds to graphite standards on ICDD (International Centre for Diffraction Data) of 01-075-1621. The peak of plane 002 indicates the aromatic conjugated-carbon bond [18] with layered structures. Due to this nature, the presence of plane 002 is used widely to monitor the conversion of graphite into GO material. From Fig. 1, it can be seen that when graphite is oxidized using a sufficient amount of permanganate, the principal peak at ~26° will shift to a smaller 2θ of around 9–10°. XRD data interpretation has been compiled in Table 1. By using the Bragg equation (Eq. (1)), we could see that the interlayer spacing (d) between the graphene layer significantly changed from 0.34 nm in graphite to 0.8–0.9 nm in GO. Such a difference is caused by the presence of oxygen-containing groups in GO material [19-20]. The introduction of oxygen functional groups between the graphene layer of GO will increase the d-spacing.

$$n\lambda = 2d\sin\theta \quad (1)$$

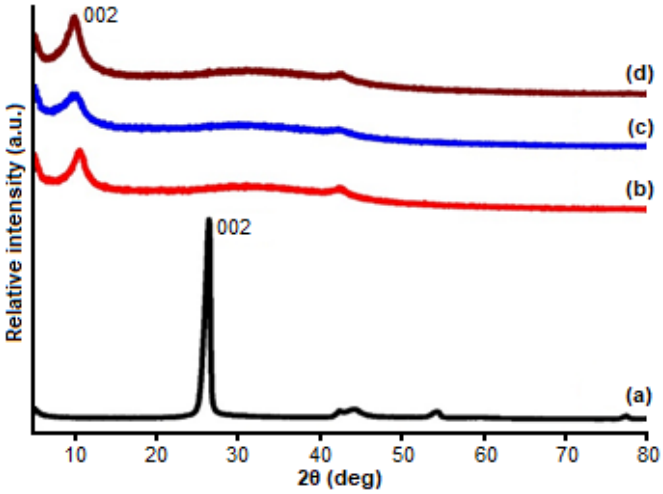

Fig 1. XRD patterns of (a) Graphite, (b) GO-5, (c) GO-6, (d) GO-7

Table 1. XRD data interpretation of all materials

No.	Material	Peak (002)					Peak (100)			
		2θ (deg)	d (nm)	FWHM	H (nm)	n	2θ (deg)	d (nm)	FWHM	D (nm)
1	Graphite	26.213	0.340	0.744	10.963	32	42.327	0.213	0.458	38.027
2	GO-5	10.487	0.843	1.603	4.977	5-6	42.404	0.213	1.183	14.726
3	GO-6	9.916	0.891	2.030	3.928	4-5	42.216	0.214	1.384	12.579
4	GO-7	9.888	0.894	1.675	4.761	5-6	42.573	0.212	0.967	18.026

where n is the order of diffraction (1), λ is X-ray wavelength (spectrum Cu Kα of 0.154 nm), d is the distance between lattice plane (nm), θ is diffraction angle.

By utilizing the Debye-Scherrer equation (Eq. (2)) from peak 002 and 100, we could calculate the height of the stacking layer (H) and the average diameter of the stacking layer (D), respectively. From the H value, we could estimate the number of graphene layers (n = H/d). The dimensions of the plane of each material can also be evaluated from D × H calculation [21]. Graphite has a field dimension of 38 × 11 nm with several layers of 32 pieces, GO-5 has a field dimension of 15 × 5 nm with some layers of 5–6 pieces, GO-6 has a field dimension of 16 × 4 nm with many layers of 4–5 nm, and GO-7 has dimensions 18 × 5 nm field with several layers 5–6 nm. The higher the oxidation level, the resulted layer will be lower. This can be understood due to the nature of permanganate oxidation is to exfoliate the graphene layers from graphite structure. The visualization of the change in the structure of graphite to graphene oxide has been presented in Fig. 2.

$$D = \frac{K\lambda}{B\cos\theta} \qquad (2)$$

where D for plane 100, H for plane 002 is crystallite size (nm), K is constant (Scherrer constant (0.9) for plane 002, Warren constant (1.84) for plane 100), λ is X-ray wavelength (spectrum Cu Kα of 0.154 nm), B is Full Width at Half Maximum (FWHM) value (radian), and θ is diffraction angle (radian).

Fourier Transform Infra-Red Spectrophotometry Analysis

Fig. 3 displays the IR spectrum of graphite and GO samples. In the graphite spectrum, there are no peaks except for a very weak peak at 3402.58 cm^{-1} [22]. This peak designates the presence of O–H groups in graphite, which usually comes from dissolved water molecules [23]. Meanwhile, all GO materials revealed characteristic peaks of oxygen-containing groups. These characteristic peaks include strong intensity at wavenumbers of ~3400 for O–H, the weak intensity at ~2800 for C–H sp^3, the weak intensity at ~1700 for C=O, the medium intensity at ~1500 for C=C of aromatic carbon, the weak intensity of ~1300 for C–O–C of ether and ester, and weak intensity

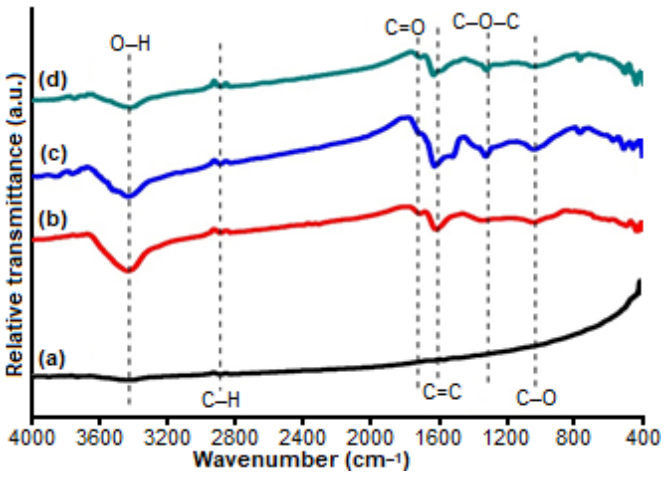

Fig 3. FTIR spectra of (a) Graphite, (b) GO-5, (c) GO-6, (d) GO-7

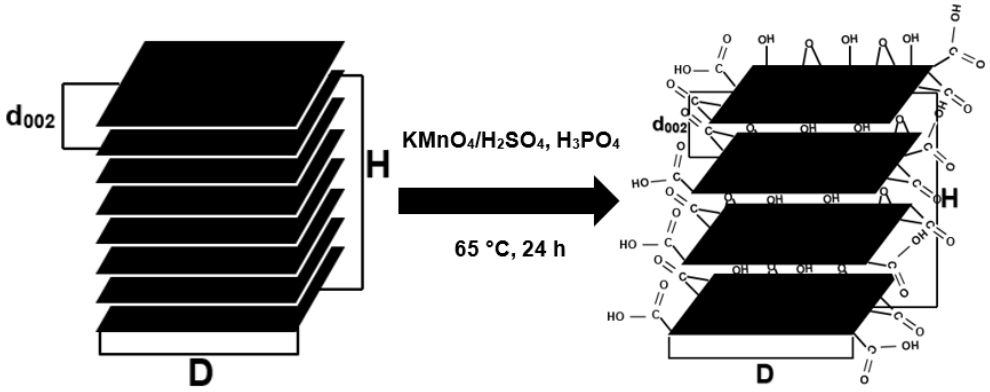

Fig 2. Visualization of changes in the structure of graphite to graphene oxide

of ~1000 for C–OH for carboxylic acids and alcohols as the previous work report [7]. The presence of these oxygen groups explained the shifting of plane 002 of graphite and GO, which is resulted from the increase of d-spacing due to the introduction of oxygen groups into graphene layers. All GO materials also contain C=C aromatic bonds in the ~1500–1600 cm^{-1} region because this material mostly contains sp^2-hybridized carbon bonds, and a few regions contain sp^3-hybridized carbon bonds due to the presence of oxygen. Looking at all the peaks of absorption of the oxygen functional groups that arise, we conclude that these peaks generally have not significantly different intensities. For a detailed interpretation of FTIR data, see Table 2.

Energy-Dispersive X-ray Spectroscopy Analysis

EDX analysis was conducted to determine the elemental content in the GO material that had been synthesized. As shown in Fig. 4, graphite powder only contains the element carbon. After the graphite was oxidized using $KMnO_4$, the carbon content decreases, and the oxygen content appears, which indicates the success of the oxidation reaction. Based on the data in Table 3, it can be concluded that the more permanganate is added to graphite, the oxidation level (ratio O/C) will also increase. The presence of impurities in the form of Na content in GO-5 of 6.45%, GO-6 of 0.50%, and GO-7 of 23.03% was derived from the PBS involved in the process of washing the material.

Selected Area Electron Diffraction Analysis

SAED is utilized to confirm the polycrystalline properties of a nanomaterial. This nature is characterized by the presence of diffraction rings that

Table 2. FTIR data interpretation of all materials

No	Material	Wavenumber of bond type (cm^{-1})					
		O–H	C–H	C=O	C=C	C–O–C	C–OH
1	Graphite	3402.58	-	-	-	-	-
2	GO-5	3427.65	2889.49	1712.86	1619.31	1350.23	1054.14
3	GO-6	3414.15	2890.45	1627.03	1521.90	1326.12	1036.78
4	GO-7	3409.33	2881.77	1713.83	1631.85	1320.33	1043.53

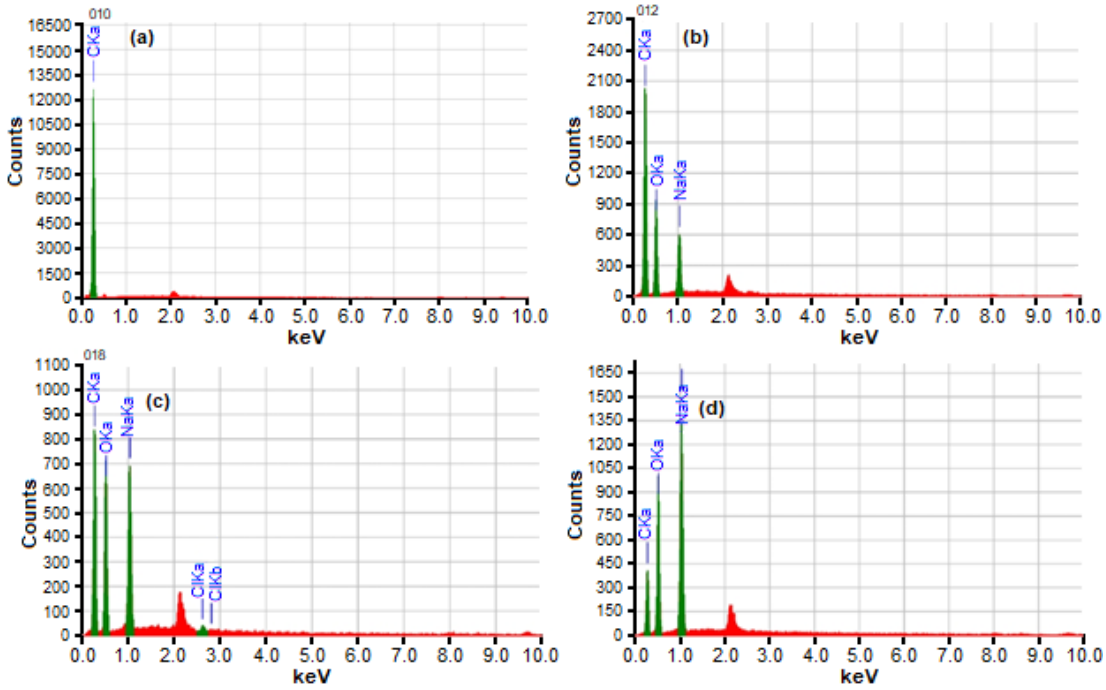

Fig 4. EDX spectra of (a) graphite, (b) GO-5, (c) GO-6, (d) GO-7

Table 3. Oxidation level of all materials

No	Material	Mass % of O	Mass % of C	Ratio O/C
1	Graphite	0	100	0
2	GO-5	37.49	56.06	0.67
3	GO-6	41.04	46.58	0.88
4	GO-7	46.24	30.73	1.50

appear. The SAED pattern of the synthesized GOs is shown in Fig. 5. From the pattern above, all GO materials revealed a polycrystalline structure with low crystallinity as denoted by the obscurity of the ring lines, in line with previous results [21]. This is likely rendered by the presence of oxygen functional groups attached to the graphene stacking layer containing sp^2 hybridized-carbon, resulting in defects in crystals with the emergence of new sp^3 carbon hybridization [24]. Graphite has polycrystalline properties with very high crystallinity and bright diffraction rings. According to calculations on the SAED pattern, after oxidation of graphite is executed, the distance between the graphite layers becomes wider. This result has been listed in Table 4. Based on the calculation results using SAED, the d-spacing of GO has a value close to 0.8 nm in the crystal plane of 002 and around 0.2 nm in the crystal plane of 100, which confirms the d-spacing calculation using XRD. We could see a slightly different value of d-spacing obtained from SAED and XRD analysis. The difference may arise from the different sizes of analysis. As we have known, SAED analysis is carried out in a focused area with several hundred nanometers in size, whereas XRD typically samples areas that cover several centimeters of a bulk sample.

Scanning Electron Microscopy Analysis

The surface morphology of the GO material was analyzed using SEM. Based on Fig. 6, Graphite shows large

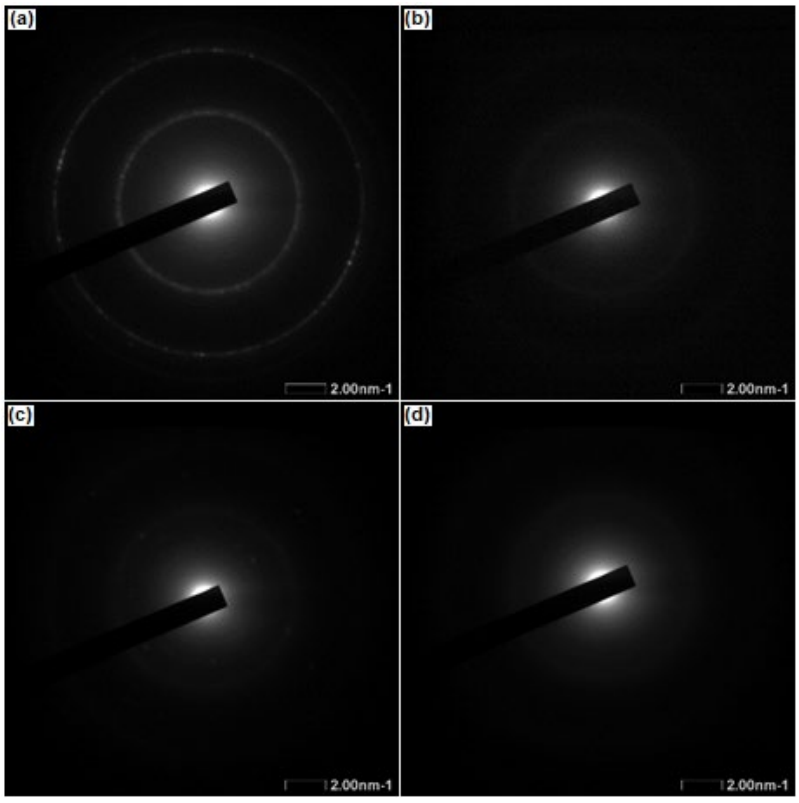

Fig 5. SAED pattern of (a) Graphite, (b) GO-5, (c) GO-6, (d) GO-7

Table 4. SAED pattern analysis of all materials

No	Materials	d (nm) Peak 002	d (nm) Peak 100
1	Graphite	0.302	0.156
2	GO-5	0.768	0.199
3	GO-6	0.756	0.218
4	GO-7	0.772	0.243

chunks with a rough and crumpled surface. GO-5 and GO-6 materials have a morphology similar to the appearance of an exfoliated layer with a wrinkled and irregular surface. In comparison, GO-7 displays a morphology like a lot of small gravel, indicating excessive oxidation reactions.

Transmission Electron Microscopy Analysis

TEM images are applied to evaluate the morphology of each material (Fig. 7). According to the literature, the permanganate provides a product with wrinkled structures, while the chlorates lead to the synthesis of graphite oxide with the planar structure of the material [25]. These images have bright and dark areas. The dark region indicates the stack layer, which has not been exfoliated or has a small distance between layers due to the lack of oxygen functional groups entering the layers. Meanwhile, the bright area shows the layer which has been successfully exfoliated [16]. Graphite has a stacked sheet structure; this indicates its nature, which contains a graphene multilayer. For GO-5, the material exhibits the presence of long and fine sheets are folded together. Meanwhile, for GO-6 and GO-7, both appear to have a thin layer that is rather wide with slightly different transparency. Although there are slight differences in transparency and the resulting layers, most of the structures of these three materials are classified as having similar nanostructures that support the d spacing data on XRD and SAED and the intensity of oxygen function absorption on FTIR.

UV-Visible Spectrophotometry Analysis

UV-Visible spectra of various GO are disclosed in Fig. 8. GO has two characteristic absorption bands on UV-Visible spectra. The central peak at a wavelength of

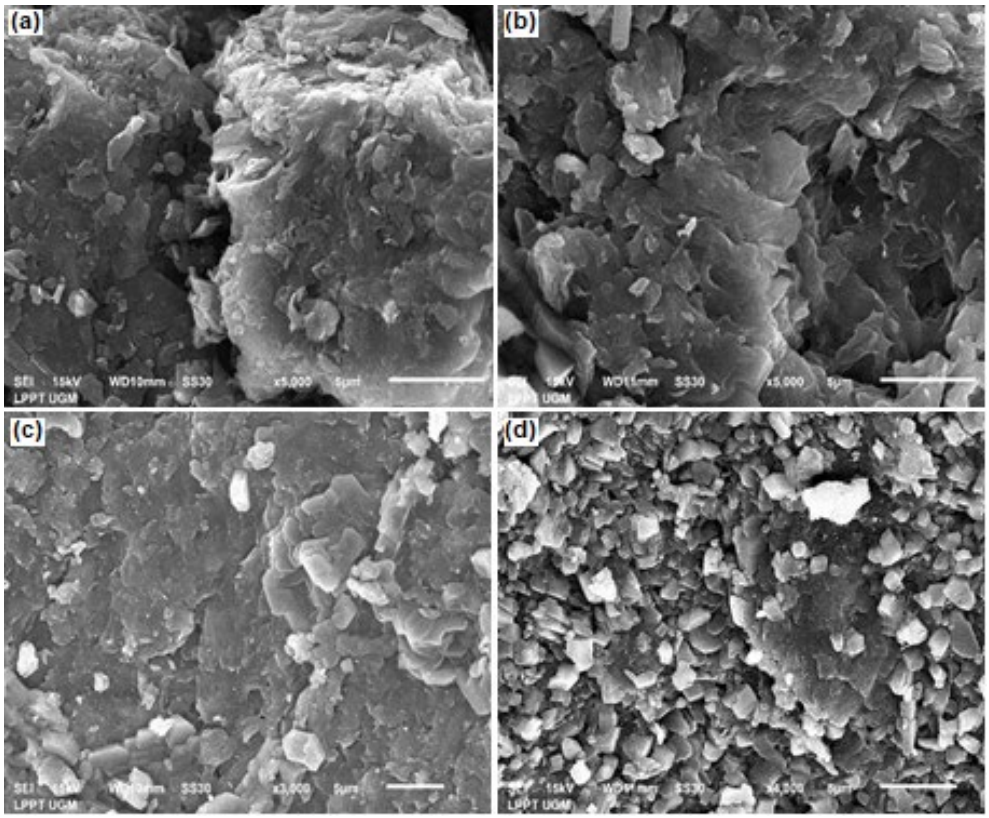

Fig 6. SEM images of (a) Graphite, (b) GO-5, (c) GO-6, (d) GO-7

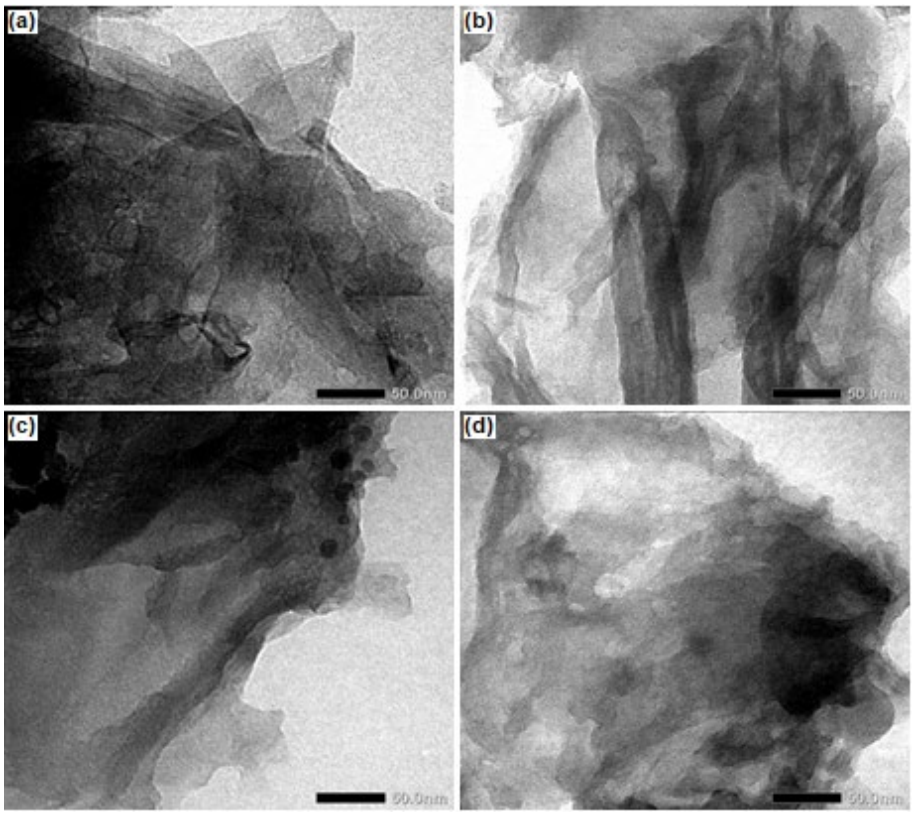

Fig 7. TEM images of (a) Graphite, (b) GO-5, (c) GO-6, (d) GO-7

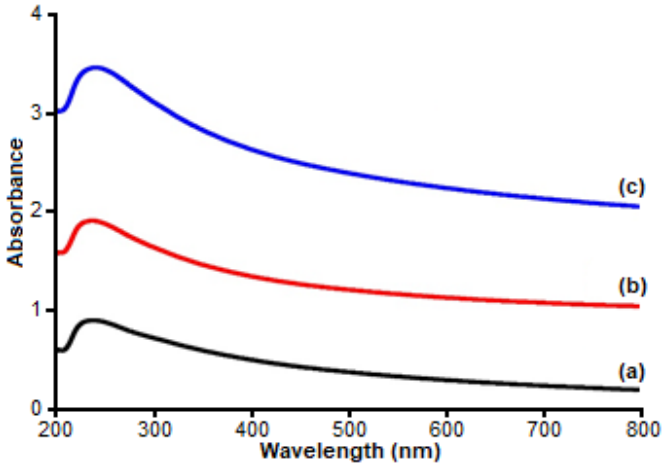

Fig 8. UV-Vis absorption spectra and visual appearances of (a) GO-5, (b) GO-6, (c) GO-7

230–240 nm correlated to the transition π→π* of the aromatic C=C bond and the shoulder peak at a wavelength of 290–300 nm, which is responsible for the n→π* transition of the C=O bond [26]. Unfortunately, we could not show UV-Vis spectra of graphite due to the non-polar characteristic, which inhibiting the solution preparation for analysis.

We also evaluate the band gap energy values on the resulted GO materials to determine the optoelectronic properties. Optical band gap energies of GO were estimated using the Tauc plot as presented in Fig. 9, following Eq. (3):

$$(\alpha h\nu)^{1/m} = A(h\nu - Eg) \quad (3)$$

where α is absorption coefficient, hν is photon energy, A is constant, Eg is band gap energy, and m is nature of transition, m = 1/2 for direct allowed transitions.

Graphite is known as a conductor with a band gap of about zero eV [27-28]. Following the oxidation from GO, we could see an increase in band gap values to approximately 3 eV. The increase in band gap value is caused by oxygen molecules on the surface. It has been reported that the greater d-spacing between graphene layers will limit the overlap of p orbitals, thereby reducing the effectiveness of the conjugate length of the π bond [29]. Furthermore, the oxygen functional group with sp^3 hybridization could results in structural changes

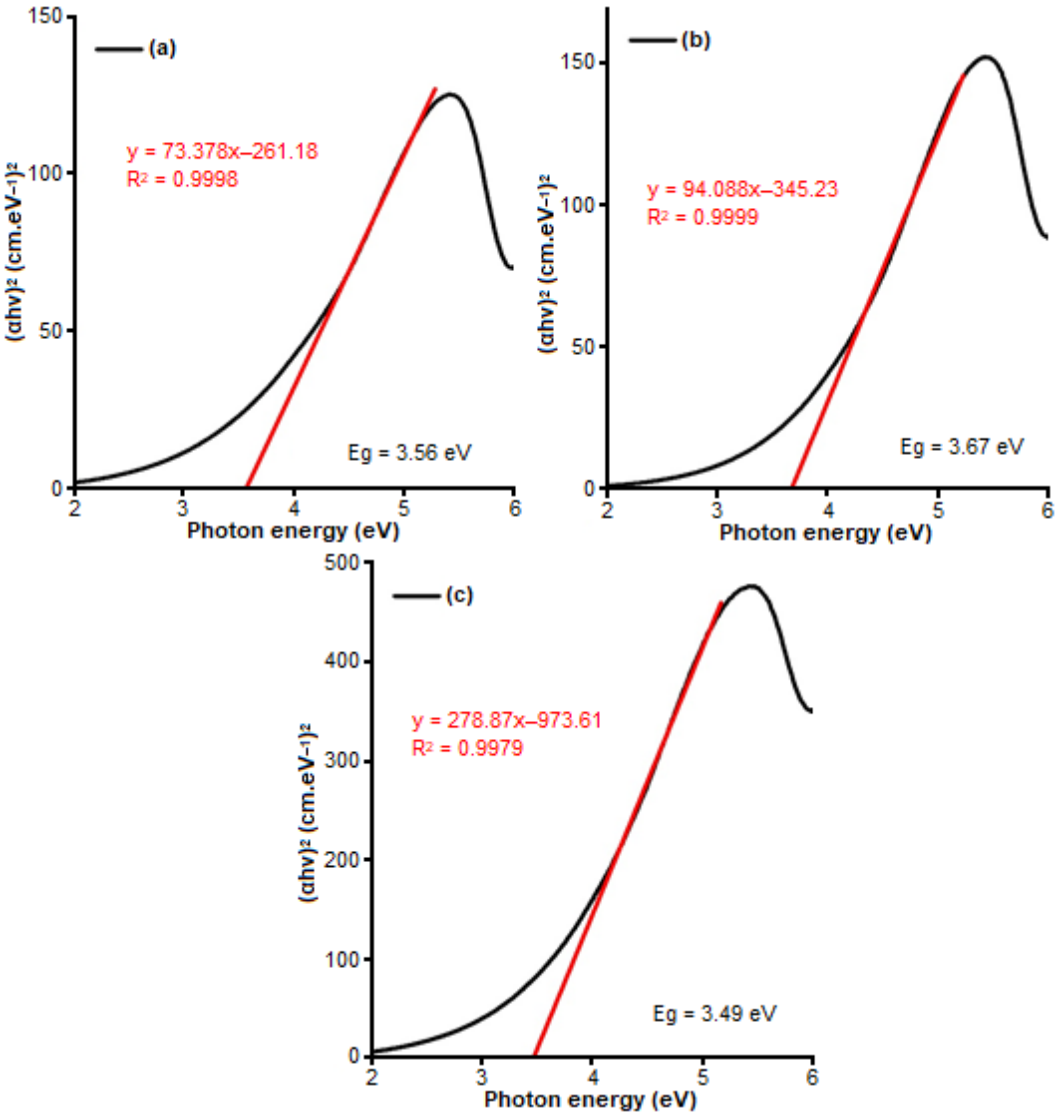

Fig 9. A Tauc plot of (a) GO-5, (b) GO-6, (c) GO-7

on the GO surface so that it disrupts the flow of electrons, thus limiting the electronic conduction. Therefore, we may say that the presence of oxygen functional groups reduces the electrical properties of GO, as evidenced by the increase in the value of the band gap [30]. However, we could not see any significant difference in band gap value to the number of oxidants. This may suggest that the oxidant ratio we used in this report is not significantly affecting to amount of oxygen functional groups as supported by the similarity of FTIR results. The use of FTIR also limits our capability to distinguish the type of oxygen functional groups. With a 3 eV band gap, GO is the potential to be used as a window layer in heterojunction solar cells [31].

Based on the results and discussion above, it can be considered that GO material synthesis has been successfully carried out through several evaluations. XRD data states that the d-spacing value increases with an increasing number of permanganates added, which is also supported by SAED data. Band gap analysis of the three materials produced a value of around 3 eV confirmed by the absorption intensity of oxygen-containing groups similar in the FTIR spectra. GO with a band gap value of 3 eV is very potential for further applications in the solar cell field.

■ CONCLUSION

Research on the effect of adding permanganate to graphite has been carried out using the Improved Tour oxidation method, resulting in GO-5, GO-6, and GO-7. The results showed that the three GO materials have similar chemical properties and structures. Starting from the results of XRD analysis, the d spacing value is around 0.8 nm, while from the results of SAED, the d spacing value is approximately 0.7 nm. FTIR spectra also display typical absorption peaks of oxygen functionalized carbon at several wavenumbers with characteristic intensities. The oxidation level exhibits an increase in the O/C ratio with the addition of permanganate to graphite. The morphological structure of both SEM and TEM also indicates insignificant differences. The results of UV-Visible spectroscopy analysis denote a main peak with the highest absorbance at a wavelength of about 230 nm and the shoulder peak at a wavelength of about 300 nm. At the same time, the resulting band gap energy is around 3.5–3.7 eV. With this band gap value, GO can be utilized for further applications in the solar cell field.

■ ACKNOWLEDGMENTS

The authors thank the Ministry of Research, Technology, and Higher Education, Republic of Indonesia, for the fund through the PMDSU Research Grant 2020 (Contract Number: 3150/UN1.DITLIT/DIT-LIT/PT/2020) and also Universitas Gadjah Mada for the financial support of this work under the scheme of the *Rekognisi Tugas Akhir* (RTA) 2020.

■ REFERENCES

[1] Nika, D.L., Cocemasov, A.I., and Balandin, A.A., 2017, "Two-dimensional thermal transport in graphene" in *Thermal Transport in Carbon-Based Nanomaterials*, 1st Ed., Eds., Zhang, G., Elsevier Science, Amsterdam, Netherlands, 57–84.

[2] Khan, M., Tahir, M.N., Adil, S.F., Khan, H.U., Siddiqui, M.R.H., Al-warthan, A.A., and Tremel, W., 2015, Graphene-based metal and metal oxide nanocomposites: Synthesis, properties, and their applications, *J. Mater. Chem. A*, 3 (37), 18753–18808.

[3] Zhu, J., Duan, R., Zhang, S., Jiang, N., Zhang, Y., and Zhu, J., 2014, The application of graphene in lithium-ion battery electrode materials, *SpringerPlus*, 3 (1), 585.

[4] Nag, A., Mitra, A., and Mukhopadhyay, S.C., 2018, Graphene and its sensor-based applications: A review, *Sens. Actuators, A*, 270, 177–194.

[5] Yang, W., Ni, M., Ren, X., Tian, Y., Li, N., Su, Y., and Zhang, X., 2015, Graphene in supercapacitor applications, *Curr. Opin. Colloid Interface Sci.*, 20 (5-6), 416–428.

[6] Li, J., Zhao, Z., Ma, Y., and Qu, Y., 2017, Graphene and their hybrid electrocatalysts for water splitting, *ChemCatChem*, 9 (9), 1554–1568.

[7] Velasco-Soto, M.A., Pérez-García, S.A., Alvarez-Qiuntana, J.A., Cao, Y., Nyborg, L., and Licea-Jiménez, L., 2015, Selective band gap manipulation of graphene oxide by its reduction with mild reagents, *Carbon*, 93, 967–973.

[8] Luong, D.X., Bets, K.V., Algozeeb, W.A., Stanford, M.G., Kittrell, C., Chen, W., Salvatierra, R.V., Ren, M., McHugh, E.A., Advincula, P.A., Wang, Z., Bhatt, M., Guo, H., Mancevski, V., Shahsavari, R., Yakobson, B.I., and Tour, J.M., 2020, Gram-scale bottom-up flash graphene synthesis, *Nature*, 577 (7792), 647–651.

[9] Eswaraiah, V., Aravind, S.S.J., and Ramaprabhu, S., 2011, Top-down method for synthesis of highly conducting graphene by exfoliation of graphite oxide using focused solar radiation, *J. Mater. Chem.*, 21 (19), 6800–6803.

[10] Yi, M., and Shen, Z., 2015, A review on mechanical exfoliation for the scalable production of graphene, *J. Mater. Chem. A*, 3 (22), 11700–11715.

[11] Chowdhury, D.R., Singh, C., and Paul, A., 2014, Role of graphite precursor and sodium nitrate in graphite oxide synthesis, *RSC Adv.*, 4 (29), 15138–15145.

[12] Wang, S., Dong, Y., He, C., Gao, Y., Jia, N., Chen, Z., and Song, W., 2017, The role of sp^2/sp^3 hybrid carbon regulation in the nonlinear optical properties of graphene oxide materials, *RSC Adv.*, 7 (84), 53643–53652.

[13] Li, B., Yin, J., Liu, X., Wu, H., Li, J., Li, X, and Guo, W., 2019, Probing van der Waals interactions at two-dimensional heterointerfaces, *Nat. Nanotechnol.*, 14 (6), 567–572.

[14] Acik, M., Mattevi, C., Gong, C., Lee, G., Cho, K., Cho, K., Chhowalla, M., and Chabal, Y.J., 2010, The role of intercalated water in multilayered graphene oxide, *ACS Nano*, 4 (10), 5861–5868.

[15] Brisebois, P.P., and Siaj, M., 2019, Harvesting graphene oxide-years 1859 to 2019: A review of its structure, synthesis, properties and exfoliation, *J. Mater. Chem. C*, 8 (5), 1517–1547.

[16] Lojka, M., Lochman, B., Jankovsky, O., Jiříčková, A., Sofer, Z., and Sedmidubský, D., 2019, Synthesis, composition, and properties of partially oxidized graphite oxides, *Materials*, 12 (15), 2367.

[17] Ranjan, P., Agrawal, S., Sinha, A., Rao, T.R., Balakrishnan, J., and Thakur, A.D., 2018, A low-cost non-explosive synthesis of graphene oxide for scalable applications, *Sci. Rep*., 8 (1), 12007.

[18] Qiu, Y., Yu, Y., Zhang, L., Qian, Y., and Ouyang, Z., 2016, An investigation of reverse flotation separation of sericite from graphite by using a surfactant: MF, *Minerals*, 6 (3), 57.

[19] Kamakshi, T., Sundari, G.S., Erothu, H., and Rao, T.P., 2018, Synthesis and characterization of graphene-based iron oxide (Fe_3O_4) nanocomposites, *Rasayan J. Chem*., 11 (3), 1113–1119.

[20] Krishnamoorthy, K., Veerapandian, M., Yun, K., and Kim, S.J., 2013, The chemical and structural analysis of graphene oxide with different degrees of oxidation, *Carbon*, 53, 38–49.

[21] Wu, R., Wang, Y., Chen, L., Huang, L., and Chen, Y., 2015, Control of the oxidation level of graphene oxide for high-efficiency polymer solar cells, *RSC Adv*., 5 (61), 49182–49187.

[22] Kumar, R., Kumar, R.M., Bera, P., Ariharan, S., Lahiri, D., and Lahiri I., 2017, Temperature-time dependent transmittance, sheet resistance and bonding energy of reduced graphene oxide on soda lime glass, *Appl. Surf. Sci.*, 425, 558–563.

[23] Dimiev, A.M., and Eigler, S., 2016, *Graphene Oxide: Fundamentals and Applications*, 1st Ed., John Wiley & Son, Hoboken, New Jersey, US.

[24] Jin, Y., Zheng, Y., Podkolzin, S.G., and Lee, W., 2020, Bandgap of reduced graphene oxide tuned by controlling functional groups, *J. Mater. Chem. C*, 8 (14), 4885–4894.

[25] Hidayah, N.M.S., Liu, W.W., Lai, C.W., Noriman, N.Z., Khe, C.S., Hashim, U., and Lee, H.C., 2017, Comparison on graphite, graphene oxide and reduced graphene oxide: Synthesis and characterization, *AIP Conf. Proc.*, 1892, 150002.

[26] Chen, J., Yao, B., Li, C., and Shi, G., 2013, An improved Hummers method for eco-friendly synthesis of graphene oxide, *Carbon*, 64, 225–229.

[27] Dillon, R.O., Spain, I.L., and McClure, J.W., 1977, Electronic energy band parameters of graphite and their dependence on pressure, temperature, and acceptor concentration, *J. Phys. Chem. Solids*, 38 (6), 635–645.

[28] Gong, J.H., Lin, S.X., Li, W., and Gao, J., 2012, Difference in electronic structure between diamond and graphite, *Appl. Mech. Mater.*, 229-231, 74–77.

[29] Hunt, A., Kurmaev, E.Z., and Moewes, A., 2014, Bandgap engineering of graphene oxide by chemical modification, *Carbon*, 75, 366–371.

[30] Hasan, M.T., Senger, B.J., Ryan, C., Culp, M., Gonzalez-Rodriguez, R., Coffer, J.L., and Naumov, A.V., 2017, Optical band gap alteration of graphene oxide *via* ozone treatment, *Sci. Rep*., 7 (1), 6411.

[31] Zekry, A., Shaker, A., and Salem, M., 2018, "Solar cells and arrays: Principles, analysis, and design" in *Advances in Renewable Energies and Power Technologies*, Eds. Yahyaoui, I., Elsevier Science, Amsterdam, Netherlands, 3–56.